In-situ transformation of Co-MOF nanorods into Co_3S_4/Ni_3S_2 nanotube arrays

for electrochemical biomass upgrading

Yixuan Feng [a], Richard Lee Smith Jr[b], Junyan Fu [a], Xinhua Qi [a, *]

[a] College of Environmental Science and Engineering, Nankai University, No. 38, Tongyan Road, Jinnan District, Tianjin 300350, China
[b] Graduate School of Environmental Studies, Tohoku University, Aramaki Aza Aoba 468-1, Aoba-ku, Sendai 980-8572, Japan

[*] *Corresponding author. E-mail: qixinhua@nankai.edu.cn (X. Qi).*

Experimental section

Materials and reagents

Thioacetamide (TAA, ≥99%) was obtained from Sinopharm Ltd. Cobalt nitrate hexahydrate (Co(NO$_3$)$_2$·6H$_2$O, 99%), 5-hydroxymethylfurfural (HMF, 97%), 2-methylimidazole (2-MeIm, 98%), 2,5-furandicarboxylic acid (FDCA, 97%), 5-hydroxymethyl-2-furancarboxylic acid (HMFCA, 97%), furfural (FF, 99%), furfuryl alcohol (FFA, 97%), 2-formyl-5-furancarboxylic acid (FFCA, >98%), 2-furoic acid (FA, 98%), benzyl alcohol (BA, ≥99%), benzoic acid (≥99%) and potassium hydroxide (KOH, 95%) were purchased from Macklin Ltd. 2-formyl-5-furancarboxylic acid (FFCA, 98%) and 2,5-diformylfuran (DFF, 98%) were purchased from Aladdin Ltd. All reagents were used without further purification.

Characterization of materials

X-ray photoelectron spectroscopy (XPS) was performed on a Thermo ESCALAB Xi with Al Kα radiation and charge correction was carried out using the binding energy of C 1s (284.8 eV) as the energy standard. Morphologies of samples were observed by scanning electron microscopy (SEM, ZEISS GeminiSEM 300). Microstructures of ultrasonically exfoliated samples from NF were characterized with field-emission transmission electron microscopy (TEM, Talos F200X G2). In the HRTEM analyses, an energy dispersive X-ray spectrometer (EDS) connected to the instrument was used to determine elements of the sample. XRD patterns were obtained using an Ultima IV X-ray diffractometer with Cu-Ka radiation (Rigaku, Japan) as the X-ray tube at 40 kV and 40 mA and with a scanning rate of 4° min^{-1}.

Electrochemical measurements

All electrochemical measurements were performed on a CHI 660E electrochemical workstation with a typical three-electrode system at room temperature. HMF electrooxidation performance was measured in an H-type device being divided with a Nafion 117 membrane. The anolyte cell had 20 mL of 1 M KOH electrolyte (pH 13.6) with different concentrations of HMF (10 mM, 50 mM, 100 mM), while the catholyte cell contained 20 mL of 1 M KOH electrolyte. The Co-Ni$_3$S$_2$ nanotube arrays were supported on NF (1 × 2 cm^2) and served as the working electrode directly. Ag/AgCl and Pt foil (1 × 1 cm^2) were employed as the reference and counter electrodes, respectively. Measured potentials were converted to the RHE scale with the following equation: $E_{RHE} = E_{Ag/AgCl} + 0.059 \times pH + 0.197$. Linear sweep voltammetry (LSV) curves were recorded at a scan rate of 5 mV s^{-1} without iR compensation. The CVs with different scan rates (20, 30, 40, 50, 60) mV/s between the potential intervals of 1.07 V to 1.15 V vs. RHE were collected for calculating the double-layer capacitance (C_{dl}). Electrochemical impedance spectroscopy (EIS) tests were conducted at frequencies from 0.01 Hz to 10^5 Hz with an amplitude of 10 mV.

Product analyses

In general, 100 μL electrolyte was periodically extracted during potentiostatic electrolysis experiments and diluted to 1 mL with deionized water, followed by neutralization with a strongly acidic ion exchange resin (Dowex 50wx8-100), which was then filtered with a 0.22 μm polyethersulfone membrane. HMF, FF, and FA and their oxidation products were analyzed using high-performance liquid chromatography

(HPLC, Agilent 1260 Infinity II) equipped with an EC-C18 column (4.6 mm 150 mm, 4 mm) and the wavelength of the UV-Vis detector was set at 265 nm. A solution of 20% ammonium formate (5 mM) and 80% methanol served as mobile phase A and mobile phase B, respectively, the flow rate was 0.5 mL·min^{-1} and the column temperature was controlled at 30 °C. BA and its oxidation products were analyzed with external standard method, using gas chromatography (GC, Agilent 8600) equipped with a Rtx-1700 column (30 m × 0.25 mm, 0.25 μm) and flame ionization detector (FID). After the electrolysis reaction, the sample was neutralized with a strong acid ion exchange resin (Dowex 50wx8-100) and subsequently diluted with ethanol (chromatographic grade). Temperature program used in the GC analyses was as follows: initial temperature = 100 °C, 1 min; final temperature = 250 °C, 10 min; heating rate = 20 °C min^{-1}. The temperature of the detector was 300 °C. Before each run, the injection needle was flushed three times with ethanol (chromatographic grade) to eliminate cross-contamination.

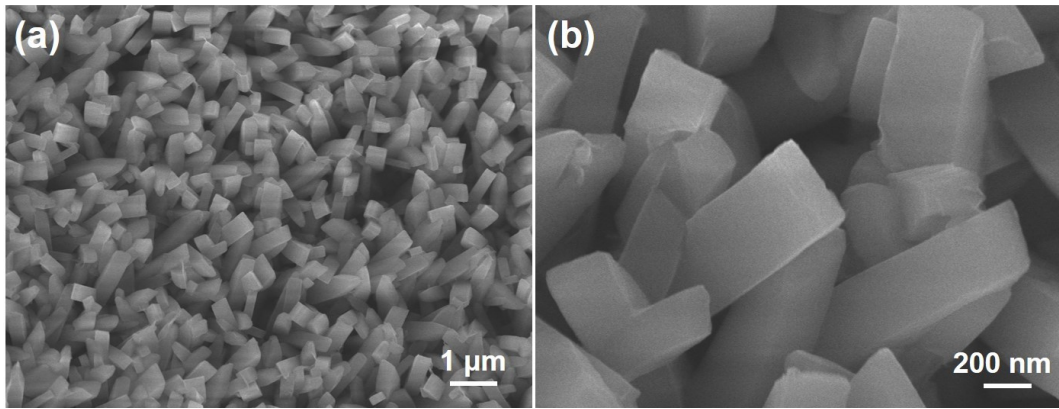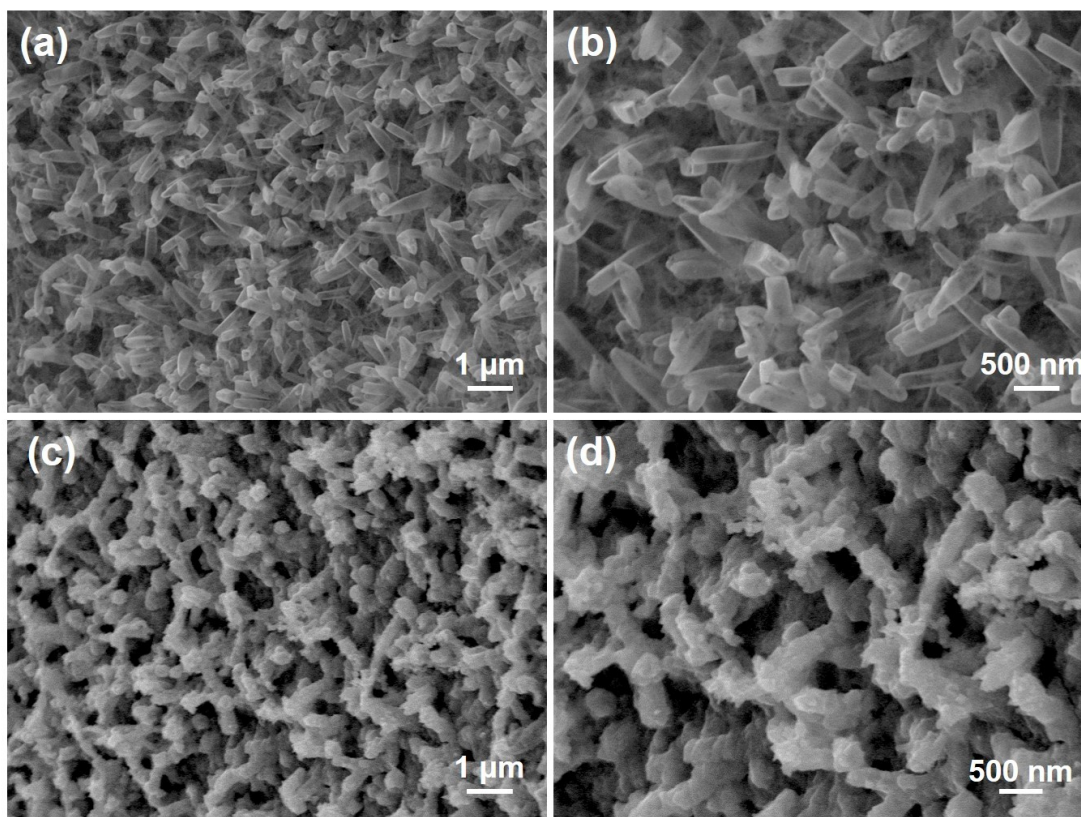Figure S1. SEM images of Co-MOF.

Figure S2. SEM images of (a, b) Co_3S_4/Ni_3S_2-1 and (c, d) Co_3S_4/Ni_3S_2-5. Suffix values -1, -3, -5 refer to solvothermal sulfurization times in hours.
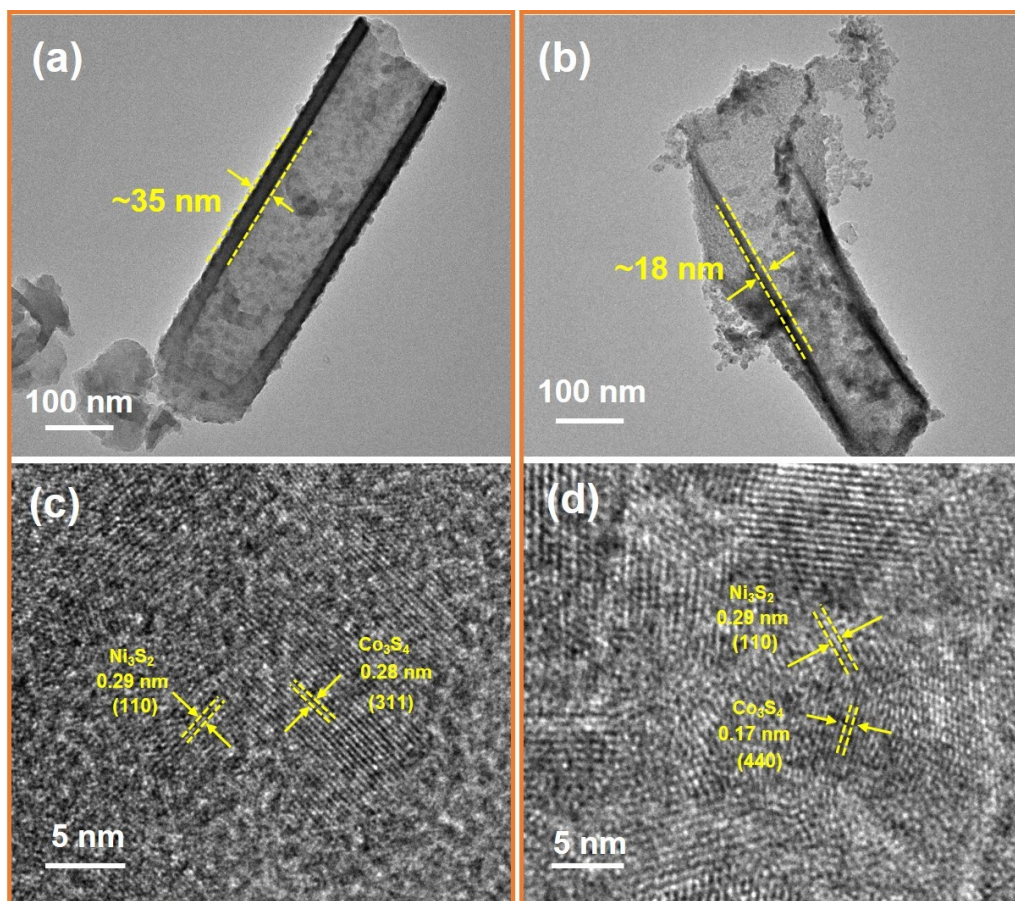
Figure S3. TEM images of (a) Co_3S_4/Ni_3S_2-1 and (b) Co_3S_4/Ni_3S_2-5; HRTEM images of (c) Co_3S_4/Ni_3S_2-1 and (d) Co_3S_4/Ni_3S_2-5. Suffix values -1, -3, -5 refer to solvothermal sulfurization times in hours
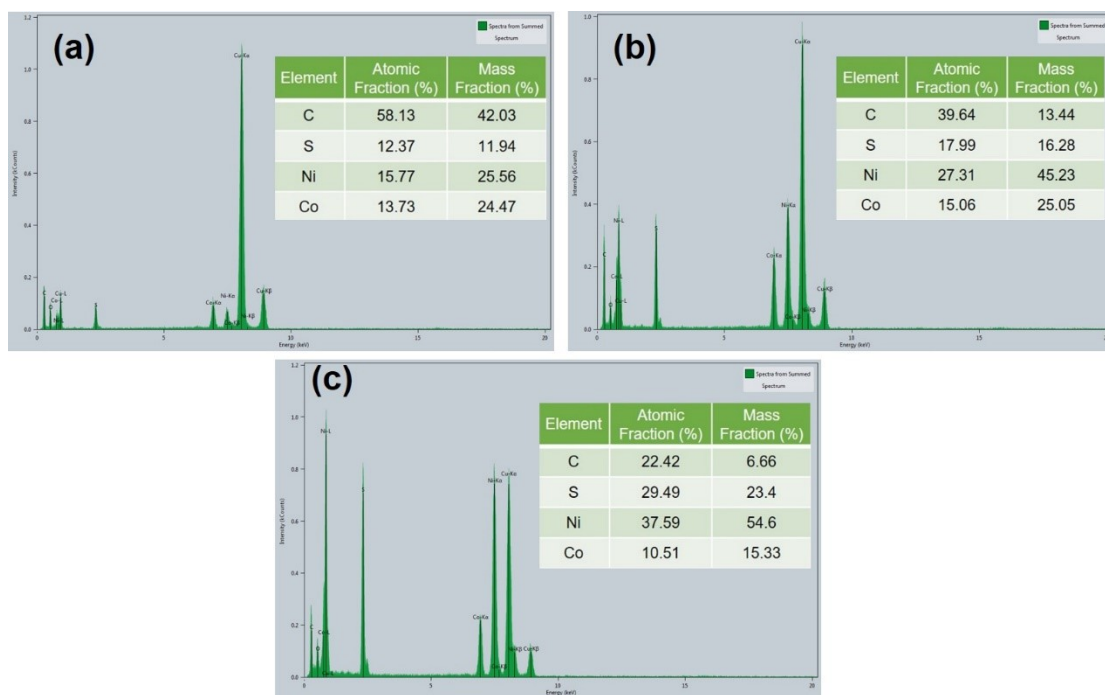
Figure S4. TEM-EDS of (a) Co_3S_4/Ni_3S_2-1, (b) Co_3S_4/Ni_3S_2-3 and (c) Co_3S_4/Ni_3S_2-5.

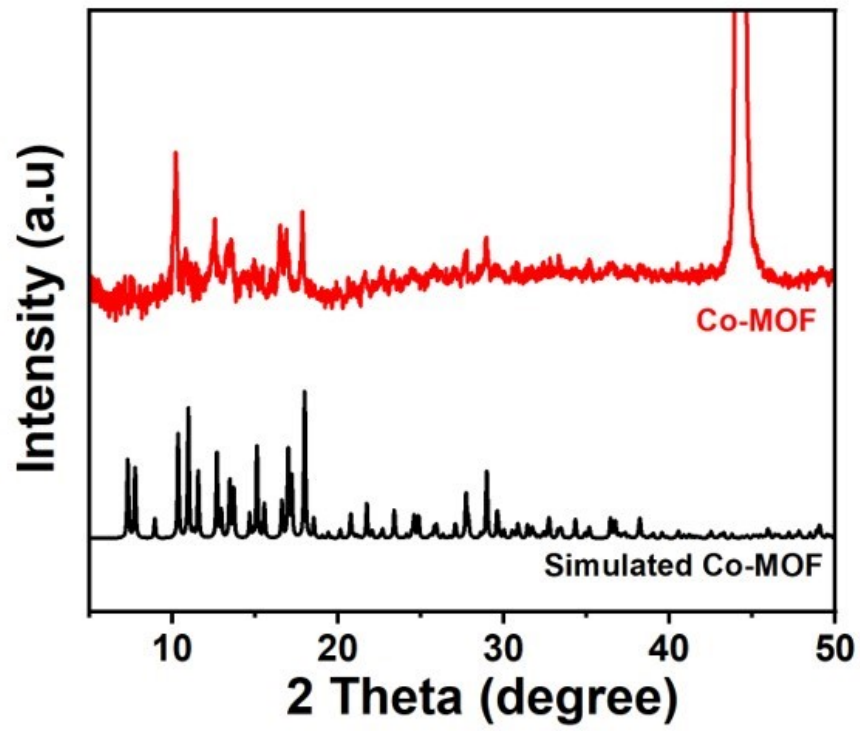Suffix values -1, -3, -5 refer to solvothermal sulfurization times in hours.
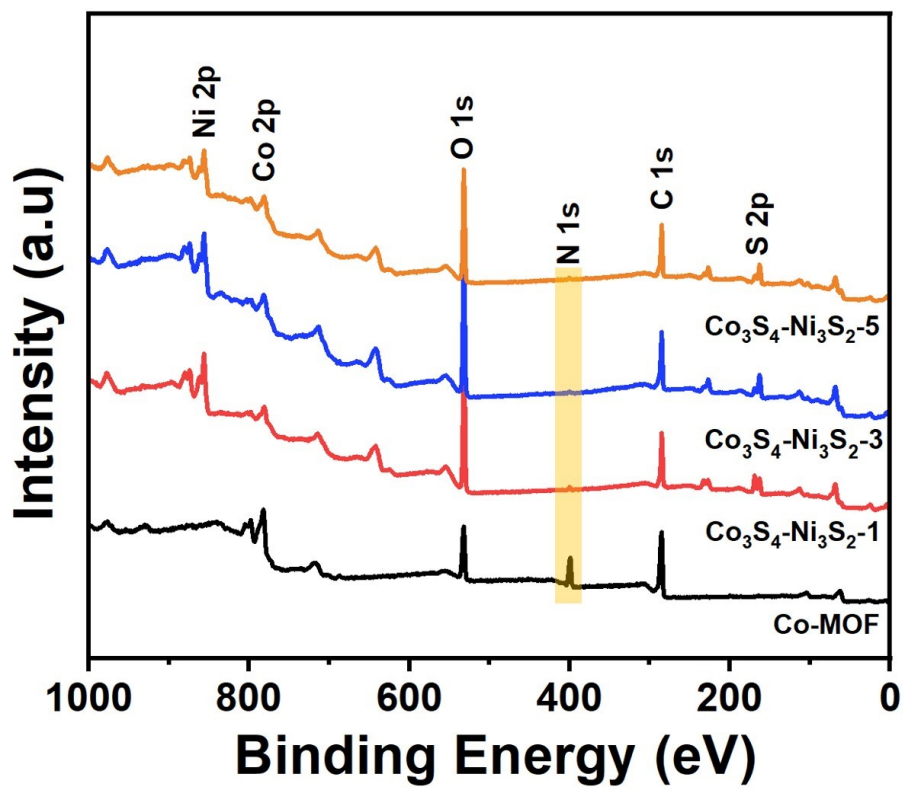
Figure S5. XRD patterns of Co-MOF.

Figure S6. XPS survey spectrum of Co-MOF and Co_3S_4/Ni_3S_2-t (t = 1 h, 3 h, 5 h).

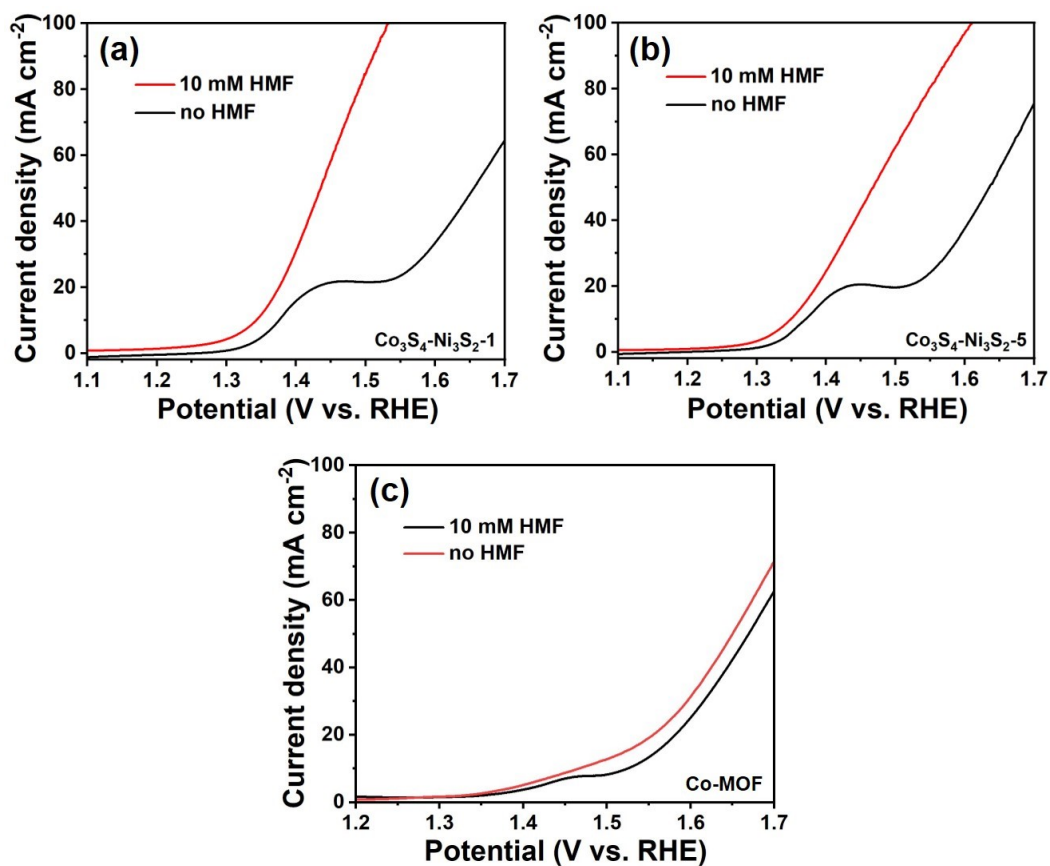Figure S7. Linear sweep voltammetry curves of (a) Co_3S_4/Ni_3S_2-1, (b) Co_3S_4/Ni_3S_2-5 and (c) Co-MOF in 1 M KOH with and without 10 mM HMF.
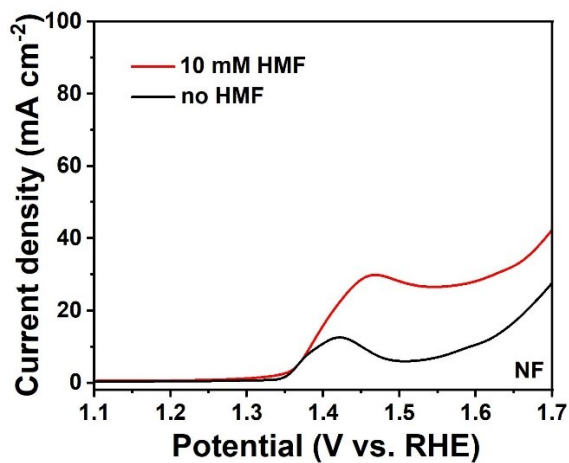

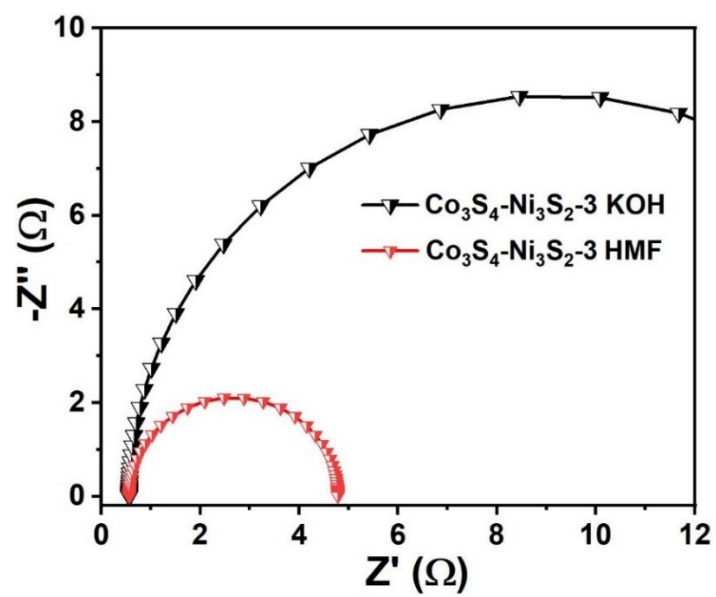Figure S8. Linear sweep voltammetry curves of nickel foam (NF) in 1 M KOH with and without 10 mM HMF.

Figure S9. Nyquist plots of Co_3S_4/Ni_3S_2-3 in 1 M KOH with and without 50 mM HMF.

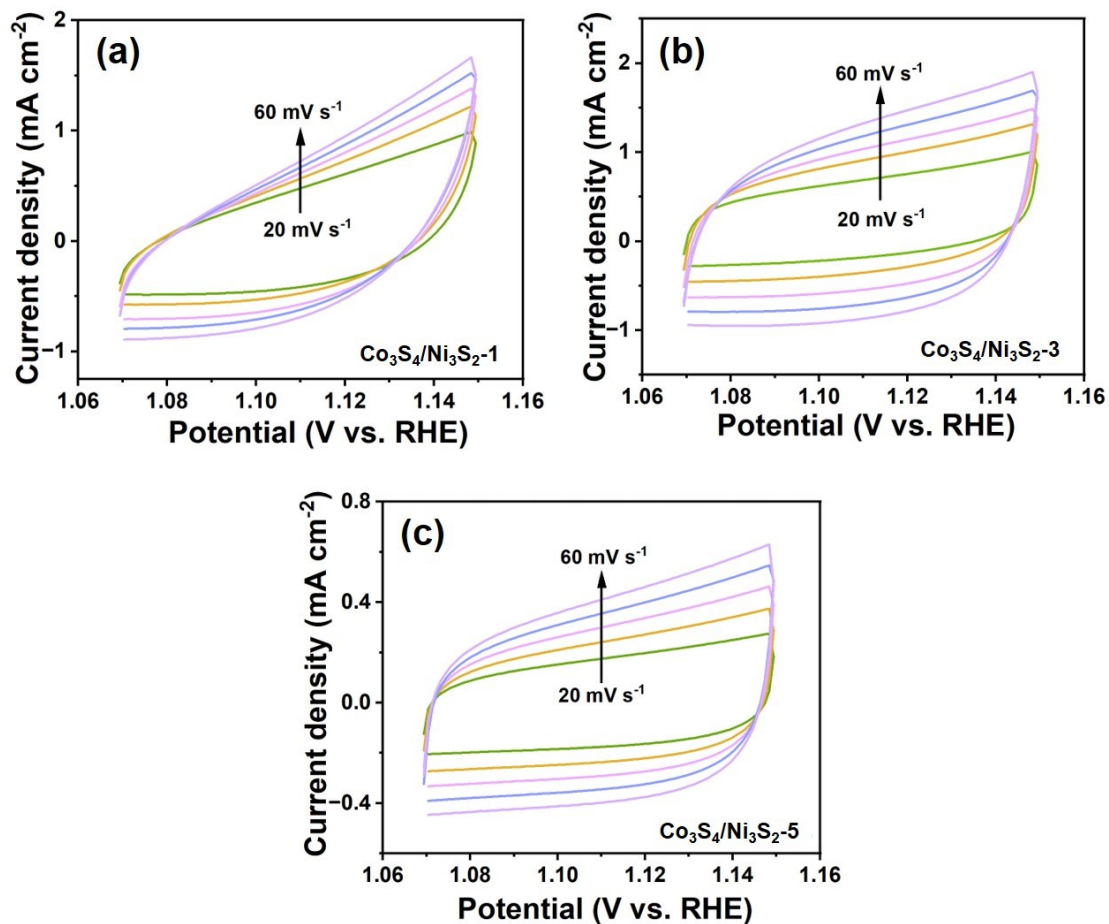Figure S10. Cyclic voltammetry curves of: (a) Co_3S_4/Ni_3S_2-1, (b) Co_3S_4/Ni_3S_2-3 and (c) Co_3S_4/Ni_3S_2-5 at different scan rates. Suffix values -1, -3, -5 refer to solvothermal sulfurization times in hours.
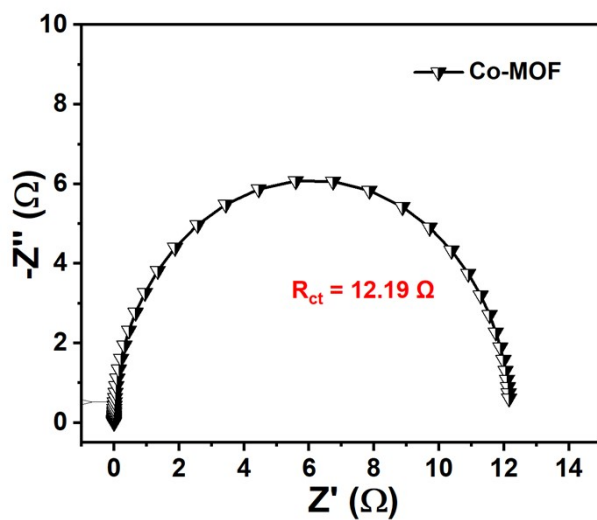
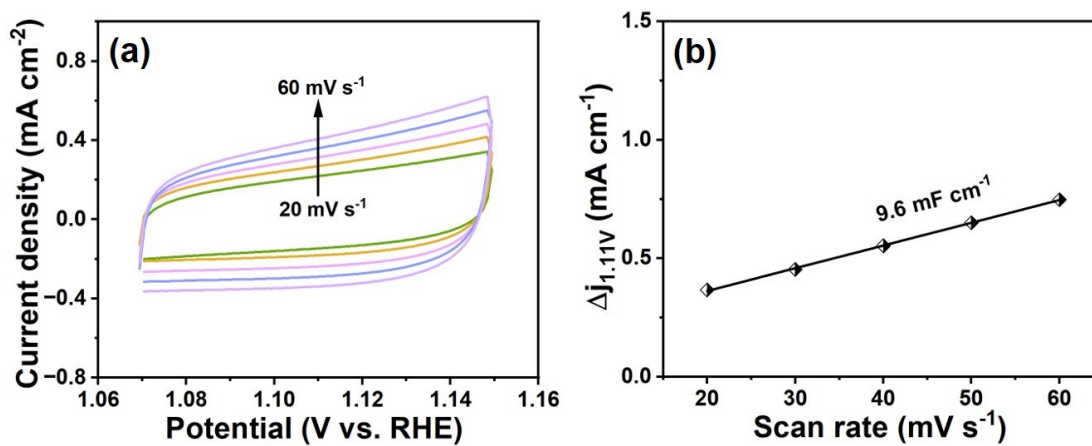Figure S11. Nyquist plots of Co-MOF in 1 M KOH with 50 mM HMF.

Figure S12. Electrochemical characterization of Co-MOF in 1 M KOH: (a) Cyclic
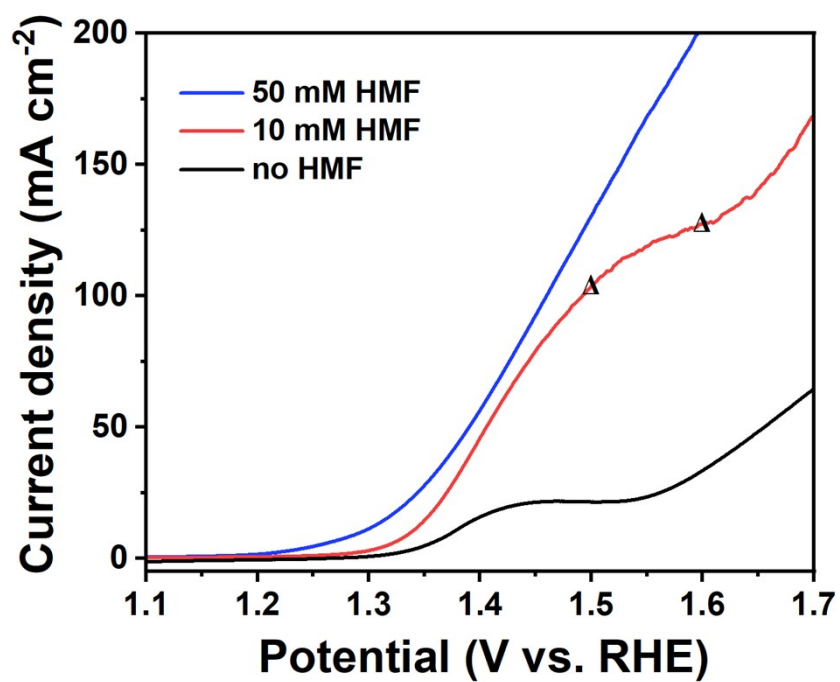
voltammetry curves and (b) capacitive currents.

Figure S13. Linear sweep voltammetry curves for Co_3S_4/Ni_3S_2 electrode in 1 M KOH

for HMF concentrations of (0, 10, 50) mM.
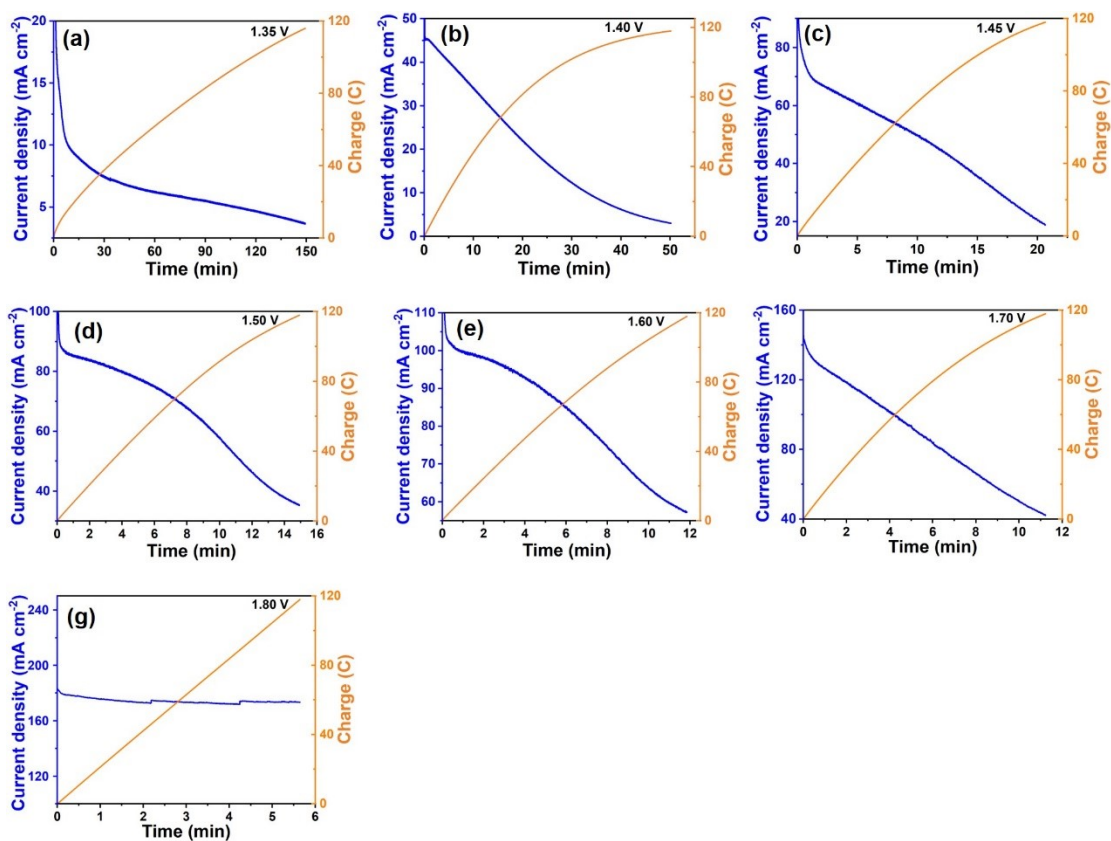
Figure S14. Current versus time and current versus charge for Co_3S_4/Ni_3S_2 electrode at different applied potentials in 1.0 M KOH for 10 mM HMF after 58 C charges were passed vs. RHE: (a) 1.35 V, (b) 1.40 V, (c) 1.45 V, (d) 1.50 V, (e)1.60 V, (f) 1.70 V and (g) 1.80 V.
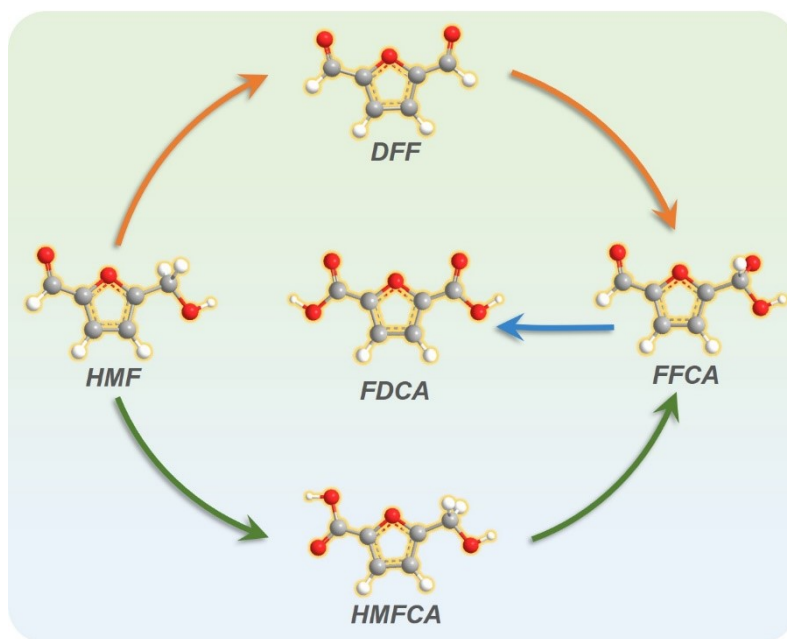
Figure S15. Two possible HMF oxidation pathways to FDCA: 5-hydroxymethyl-2-furanformic acid (HMFCA) pathway and 2,5-diformylfuran (DFF) pathway.
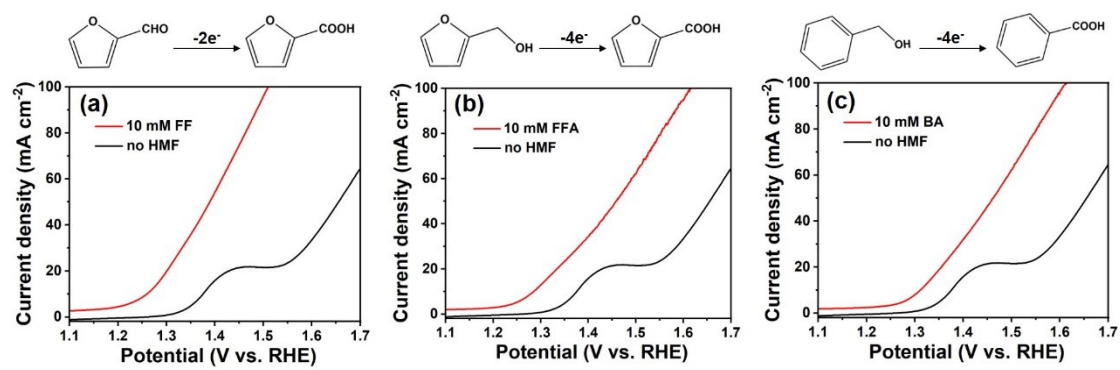
Figure S16. Linear sweep voltammetry curves of Co_3S_4/Ni_3S_2 in 1 M KOH with and without 10 mM organic substrate: (a) furfural (FF), (b) furfuryl alcohol (FFA), (c) benzyl alcohol (BA).
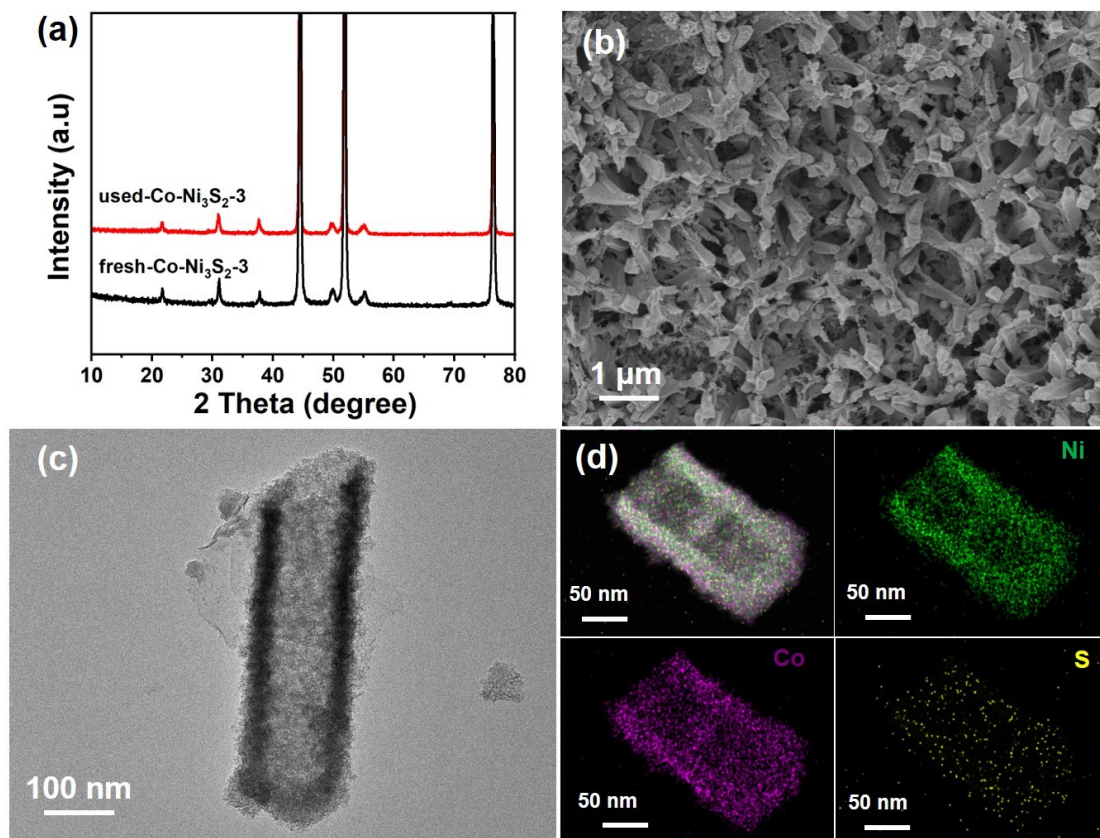
Figure S17. Crystal structure and morphological of Co_3S_4/Ni_3S_2 electrode after electrocatalytic oxidation of HMF: (a) XRD patterns, (b) SEM image, (c) TEM image and (d) TEM-EDS elemental mappings.
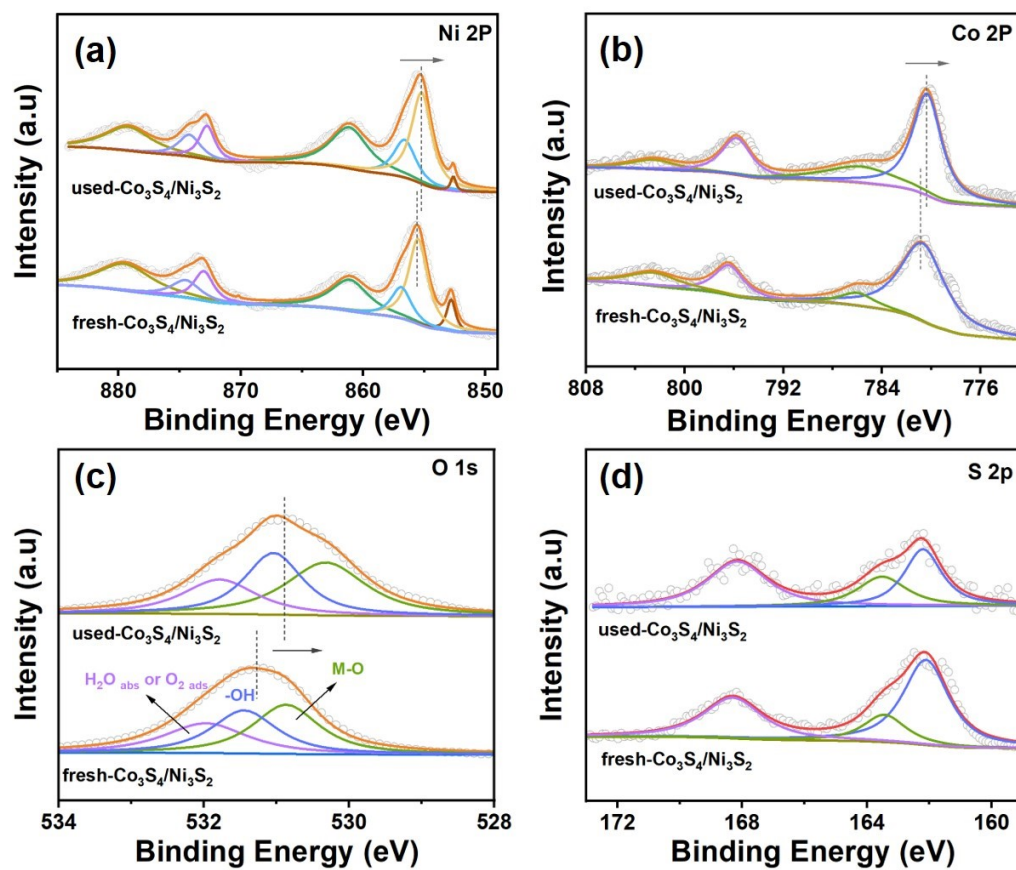
Figure S18. XPS spectrums of Ni 2p, Co 2p, S 2p and O 1s of used-Co_3S_4/Ni_3S_2 and fresh-Co_3S_4/Ni_3S_2.

Table S1. EIS fitted simulation parameters of Co_3S_4/Ni_3S_2-1, Co_3S_4/Ni_3S_2-3 and Co_3S_4/Ni_3S_2-5.

Samples	R_{ct} (Ω)	R_s (Ω)	C_{dl} (F)
Co_3S_4/Ni_3S_2-1	4.53	2.59	1.65
Co_3S_4/Ni_3S_2-3	4.08	1.37	2.07
Co_3S_4/Ni_3S_2-5	5.04	9.30	2.62

Table S2. Performance of Co_3S_4/Ni_3S_2-3 electrode developed in this work (*) and literature reported materials for oxidation of 5-hydroxymethylfurfural (HMF) to 2,5-furandicarboxylic acid (FDCA) showing applied potentials and faradaic efficiencies (FE).

Electrode Material	Electrolyte	HMF Conc. (mM)	Applied potential (V vs. RHE)	FDCA yield (%)	FE of FDCA (%)	Ref.
Co_3S_4/Ni_3S_2	1 M KOH	10	1.43	~100	~100	This work
Co_3S_4/Ni_3S_2	1 M KOH	50	1.43	98.5	97.2	This work
Co_3S_4/Ni_3S_2	1 M KOH	100	1.43	91.8	90.2	This work
NiO-CMK-1	0.2 M KOH	20	1.73	-	51.4	1
NiCoBDC-NF	0.1 M KOH	10	1.55	99	78.8	2
NiCoFe-LDHs	1 M NaOH	10	1.52	~82	-	3
P-HEOs/CP	1 M KOH	10	1.50	97.4	96.6	4
$NiCo_2O_4$	1 M KOH	5	1.50	72	80	5
d-NiFe LDH/CP	1 M KOH	10	1.48	96.8	84.5	6
NiS_x/Ni_2P	1 M KOH	10	1.46	98.5	95.1	7
$Ni_{0.9}Cu_{0.1}(OH)_2$	1 M KOH	5	1.45	91.2	91.2	8
$CoO-CoSe_2$	1 M NaOH	10	1.43	99	97.9	9
hp-Ni	1 M KOH	10	1.42	-	92−98	10
$InOOH-O_V$	1 M KOH	10	1.48	91.6	90.7	11
t-Ni1Co1-MOF	1 M KOH	10	1.40	96	96	12

Key.   CMK: carbon mesostructured from Korea; NF: nickel foam; LDH: layered double hydroxide; HEO: high entropy oxide; CP: carbon paper; hp: hierarchically porous; PBA: Prussian Blue Analogue; t: transformed; MOF: metal-organic framework.

Table S3. Electrochemical oxidation of biomass-related substrates with Co_3S_4/Ni_3S_2-3 electrode.

Electrolyte	Applied potential (V vs. RHE)	Oxidation product	Yield (%)	FE (%)
1 M KOH + 10 mM FF	1.43	FA	99.2	98.3
1 M KOH + 10 mM FFA	1.43	FA	98.7	99.0
1 M KOH + 10 mM BA	1.43	BA	98.5	96.4

Reference

1.   F. J. Holzhaeuser, T. Janke, F. Oeztas, C. Broicher and R. Palkovits, *Adv. Sustain. Syst.*, 2020, **4**, 1900151.

2.   M. Cai, Y. Zhang, Y. Zhao, Q. Liu, Y. Li and G. Li, *J. Mater. Chem. A*, 2020, **8**, 20386-20392.

3.   M. Zhang, Y. Q. Liu, B. Y. Liu, Z. Chen, H. Xu and K. Yan, *ACS Catal.*, 2020, **10**, 5179-5189.

4.   K. [Gu, D. Wang, C. Xie, T. Wang, G. Huang, Y. Liu, Y. Zou, L. Tao and S. Wang, *Angew. Chem. Int. Ed.*, 2021, **60**, 20253-20258.

5.   M. J. Kang, H. Park, J. Jegal, S. Y. Hwang, Y. S. Kang and H. G. Cha, *Appl. Catal. B*, 2019, **242**, 85-91.

6.   Y.-F. Qi, K.-Y. Wang, Y. Sun, J. Wang and C. Wang, *ACS Sustain. Chem. Eng.*, 2022, **10**, 645-654.

7.   B. Zhang, H. Fu and T. Mu, *Green Chem.*, 2022, **24**, 877-884.

8.   J. Zhang, P. Yu, G. Zeng, F. Bao, Y. Yuan and H. Huang, *J. Mater. Chem. A*, 2021, **9**, 9685-9691.

9.   X. Huang, J. L. Song, M. L. Hua, Z. B. Xie, S. S. Liu, T. B. Wu, G. Y. Yang and B. X. Han, *Green Chem.*, 2020, **22**, 843-849.

10.   B. You, X. Liu, X. Liu and Y. J. Sun, *ACS Catal.*, 2017, **7**, 4564-4570.

11.   F. Ye, S. Zhang, Q. Cheng, Y. Long, D. Liu, R. Paul, Y. Fang, Y. Su, L. Qu, L. Dai and C. Hu, *Nat. Commun.*, 2023, **14**, 2040-2040.

12.   X. Deng, M. Li, Y. Fan, L. Wang, X.-Z. Fu and J.-L. Luo, *Appl. Catal. B*, 2020,

278, 119339.